A.

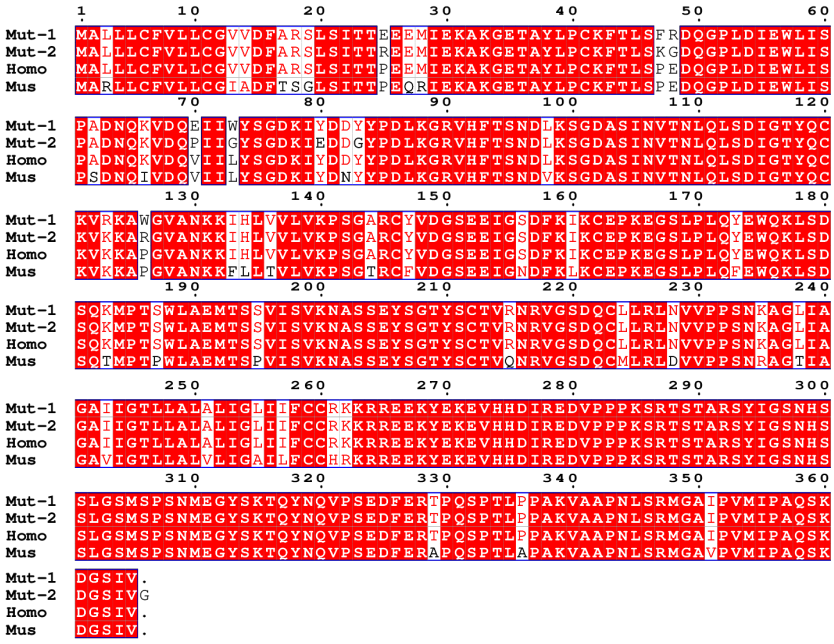

B.

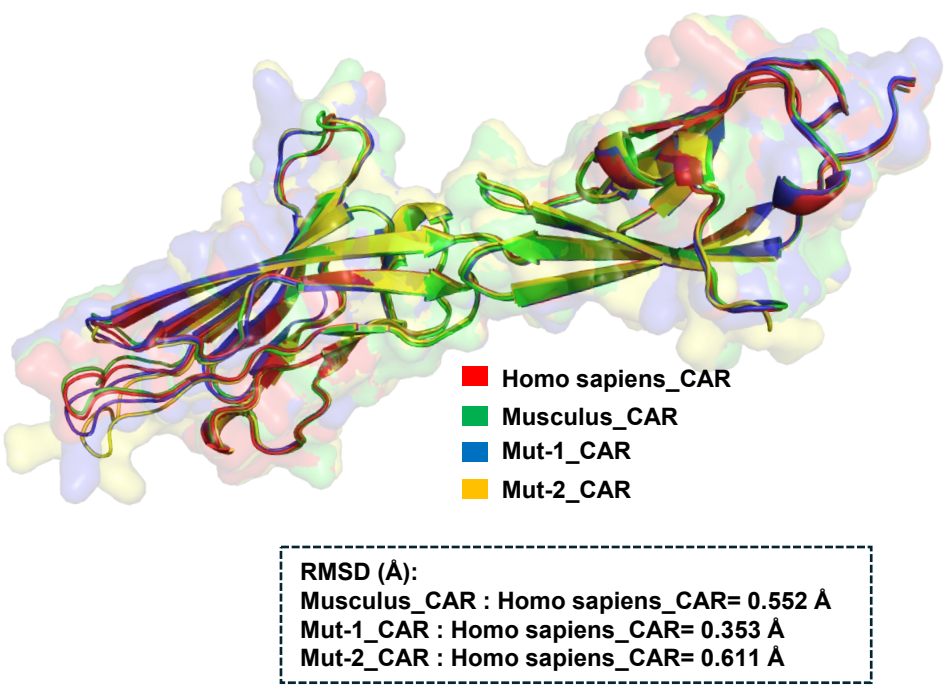

Figure S1. Sequence and structural comparison of wild-type and mutant CAR prot eins. (a) Sequence alignment of human_CAR, mouse_CAR, and two CAR mutants.(b) Structural superimposition analysis showing that the overall conformational differences a mong the four CAR variants are less than 1 Å, indicating high structural similarity.

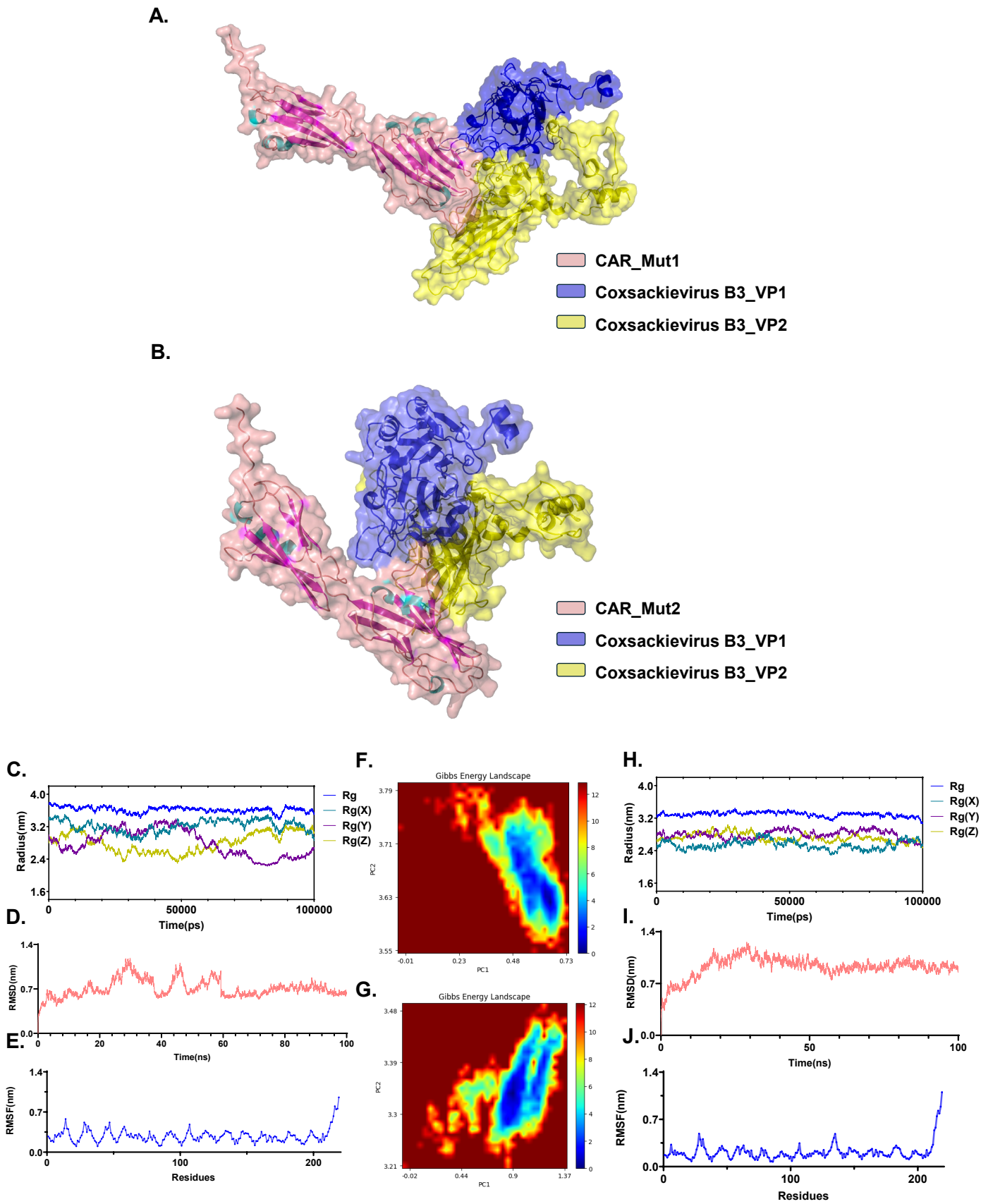

Figure S2. Molecular dynamics simulation of CAR mutants. (A–B) Structural models of the MUT-1 and MUT-2 CAR mutants in complex with the viral capsid protein.(C–F) Molecular dynamics analysis of the MUT-1 mutant, including radius of gyration (C), RMSD (D), RMSF (E), and free energy landscape (F). (G–J) Molecular dynamics analysis of the MUT-2 mutant, including free energy landscape (G), radius of gyration (H), RMSD (I), and RMSF (J).

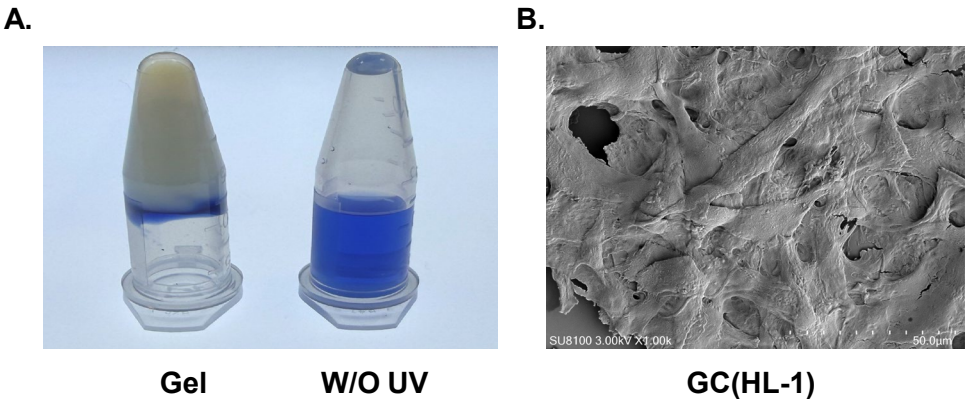

Figure S3. Characterization of hydrogel materials. (A) Photographs of hydrogels prepared from 10 wt% PEG-DA and 1 wt% I2959, before and after 15 minutes of UV irradiation (6 W). (B) Representative images showing gelled wild-type HL-1 cells encapsulated within the hydrogel matrix.

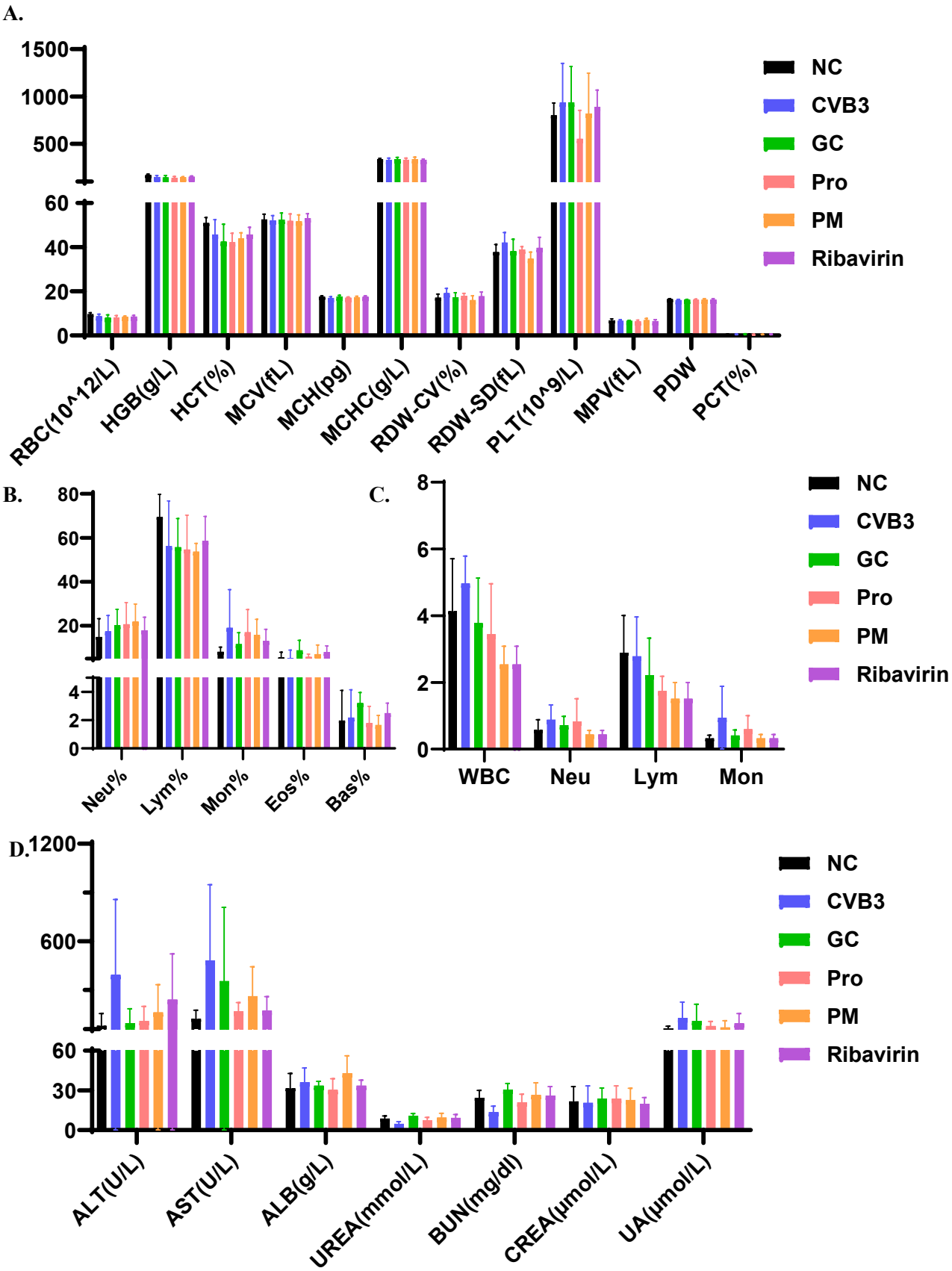

Figure S4. Hematological and biochemical assessment of mice after CVB3 infection therapy with gelled cells. (A) Complete blood count analysis;(B) Leukocyte classification;(C) Total white blood cell count;(D) Serum biochemical analysis evaluating systemic safety after treatment.

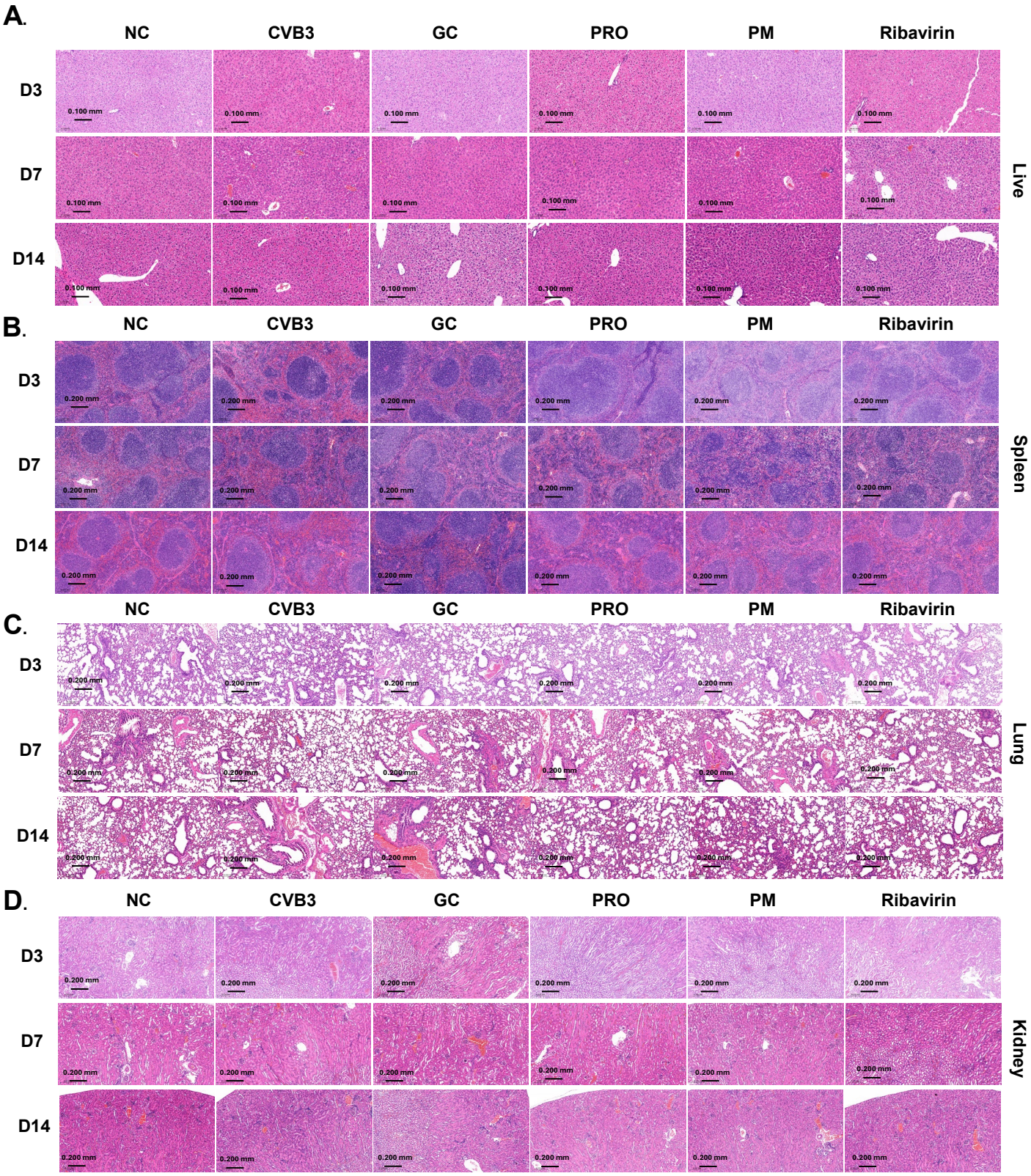

Figure S5. Histopathological analysis of major organs at days 3, 7, and 14 post-treatment; liver (A), spleen (B), lung (C), and kidney (D).

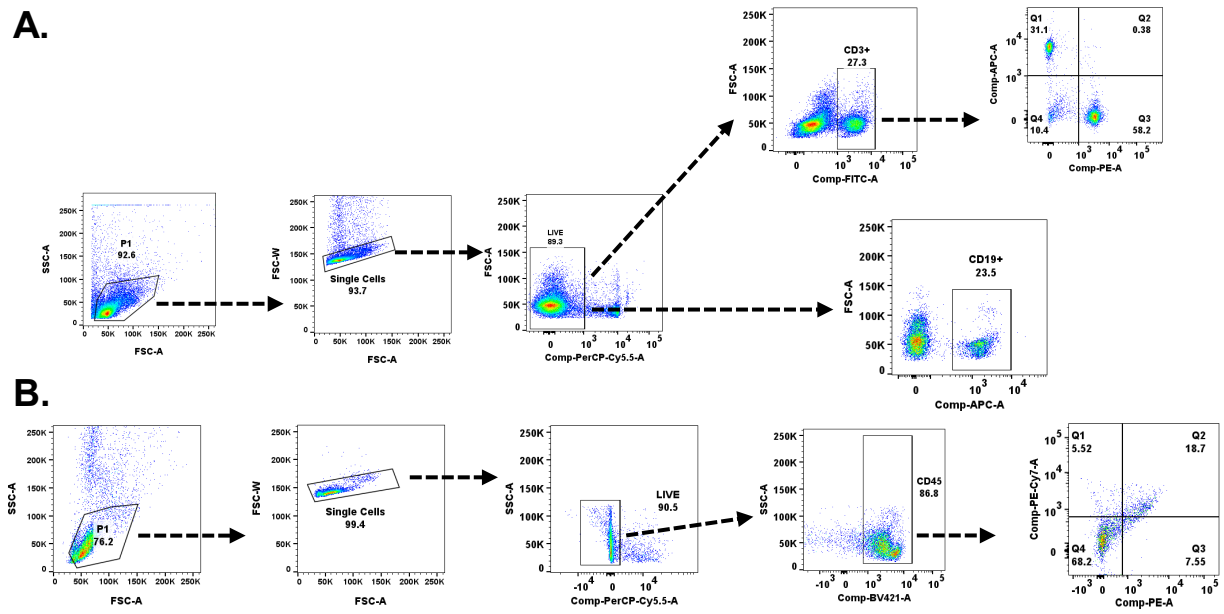

Figure S6. Gating strategies for the characterization of immune cell subsets. Flow cytometry analysis was performed on splenic leukocytes isolated 28 days post-treatment to evaluate the systemic immunogenicity of PMs. (A) Gating strategy for T cell and B cell populations. Following the exclusion of doublets and dead cells, leukocytes were identified by their characteristic forward scatter (FSC) and side scatter (SSC) profiles. T cell subsets were defined as $CD3^{+}CD4^{+}$ (helper T cells) and $CD3^{+}CD8^{+}$ (cytotoxic T cells), while B cells were identified as $CD3^{-}CD19^{+}$ populations. (B) Gating strategy for macrophage populations. Myeloid cells were initially gated based on FSC/SSC parameters, and macrophages were further identified as the $F4/80^{+}CD11b^{+}$ double-positive subpopulation。

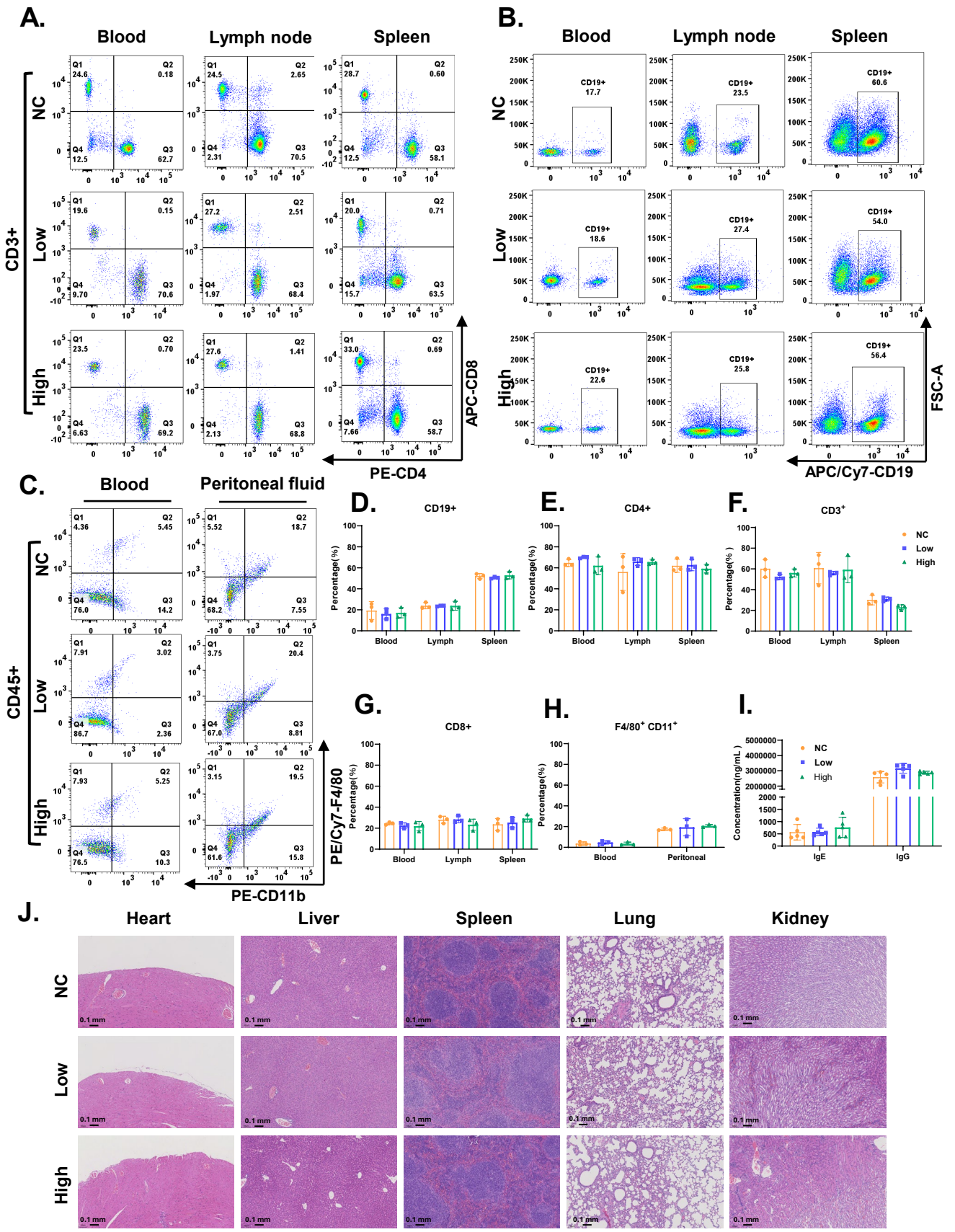

Figure S7. Long-term toxicity and immunogenicity analysis of PMs 28 days post-administration. To evaluate the chronic systemic response, comprehensive immune profiling and histological assessments were performed. (A) Representative flow cytometry plots showing the distribution of T cell subsets in the peripheral blood, lymph nodes, and spleen. (B) Representative flow cytometry plots showing the percentage of B cells across the peripheral blood, lymph nodes, and spleen. (C) Representative flow cytometry plots of macrophage populations identified in the peritoneal fluid and peripheral blood. (D–H) Quantitative statistical analysis of the proportions of T cell subsets, B cells, and macrophages in the indicated tissues. No significant differences were observed between the control and PM-treated groups ($P > 0.05$). (I) Serum levels of immunoglobulins IgG and IgE as measured by ELISA, indicating no significant systemic hypersensitivity or robust anti-drug antibody response. No significant differences were observed between the control and PM-treated groups ($P > 0.05$). (J) Representative H&E stained sections of major organs (heart, liver, spleen, lung, and kidney). Data are presented as mean ± SEM.

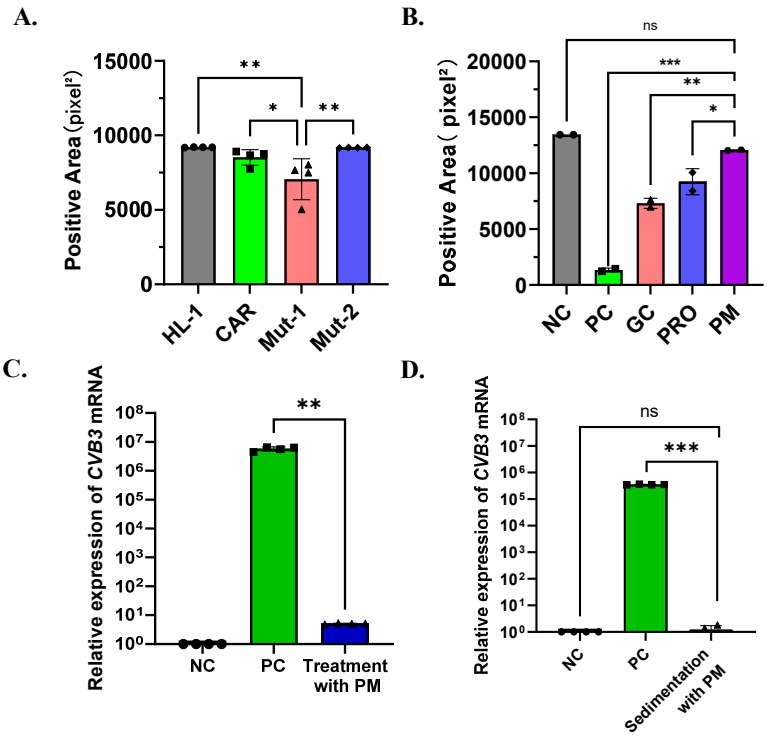

Figure S8. Viral clearance and neutralization capacity of the gelated cells. (A) Statistical analysis of viral plaque areas in four cell types (HL-1, CAR, Mut-1, and Mut-2) infected with 100 $TCID_{50}$; The Mut-1 group exhibited the most significantly enlarged plaque area.(B) Statistical analysis of HeLa cell plaque areas following treatment with three types of gelated cells; Treatment with Mut-1 resulted in the largest surviving area of HeLa cells.(C-D)100 $TCID_{50}$ of CVB3 was co-incubated with 1 × 10^6 gelated cells at 37°C for 4 hours and centrifuged at 1000 rpm for 5 min. Then, 100 μL of the supernatant(C) and the gelated cell (D) pellet were separately applied to infect HeLa cells for 24 hours. Quantitative RT-PCR analysis of intracellular CVB3 RNA levels in HeLa cells.

Table S1. Primers Used for the RT-qPCR Analysis

Target	forward	reverse
NM_021693	5'-GAGGATCCCCGGGTACCGGTCG CCACCATGCTTCTGGCCATGGTC-3'	5'-CACACATTCCACAGGCTAGTC ATATCTTGCCTCTCATCCCTCTCAT C-3'
CAR	5'-CCTCCTAAGTCCCGAACATC-3'	5'-TTGGGCAGGTATCATCACAG-3'
h-β-actin	5'-CTCTTCCAGCCTTCCTTCCT-3'	5'-AGCACTGTGTTGGCGTACAG-3'
CVB3	5´-CGGTACCTTTGTGCGCCTGT-3´	5´-CAGGCCGCCAACGCAGCC-3´

Table S2. List of antibody

Antibody	Clone	IDENTIFIER	Source
anti-mouse CD3 FITC	Clone: BY17A2	Cat. No. AC1102	Beyotime
anti-mouse CD4 PE	Clone: 30-F11	Cat. No. G0025	Selleck
anti-mouse CD8 APC	Clone: 53-6.7	Cat. No. G0003	Selleck
anti-mouse CD19 APC	Clone: BY1D3	Cat. No. AC0947	Beyotime
anti-mouse CD45 PB	Clone: 30-F11	Cat. No. G0025	Selleck
anti-mouse CD11b PE	Clone: M1/70	Cat. No. G4667	Selleck
anti-mouse F4/80 PE-Cy7	Clone: BM8	Cat. No. G0064	Selleck
Live/Dead 7-ADD	/	Cat. No. H9999	Selleck